Turkish Journal of Electrical Engineering & Computer Sciences

http://journals.tubitak.gov.tr/elektrik/

Research Article

Turk J Elec Eng & Comp Sci
(2017) 25: 1358 – 1374

doi:10.3906/elk-1404-545

Vector control of unbalanced 3-phase IM using forward and backward components

Mohammad JANNATI*, **Nik Rumzi NIK IDRIS**
UTM-PROTON Future Drive Laboratory, Faculty of Electrical Engineering,
Universiti Teknologi Malaysia, Johor Bahru, Malaysia

Received: 28.04.2014 • **Accepted/Published Online:** 10.05.2016 • **Final Version:** 10.04.2017

Abstract: In some industries, continuous operation of 3-phase induction motors (IMs) even under faults until the scheduled maintenance time is essential. Conventional control techniques such as field-oriented control (FOC) cannot be used to control faulty IMs since this will result in significant oscillations in the speed and torque. Consequently, a new control approach must be developed for improving IM performance during fault conditions. This paper presents a method for vector control of 3-phase IMs under open-phase faults. The main advantage of this control scheme is its ability to handle not only one phase but also two phases of open-phase fault conditions. When applying this control technique to a faulty machine, only minor changes to the parameters used in the equations are needed and the conventional FOC algorithm used for healthy 3-phase IMs can still be used. In this paper, simulation and experimental results are presented to study the effectiveness of the proposed technique to control both healthy and faulty 3-phase IMs. The results show that the proposed technique reduces electromagnetic torque pulsations during open-phase fault conditions.

Key words: Electromagnetic torque pulsations reduction, field-oriented control, forward and backward components, open-phase fault, 3-phase induction motor, vector control

1. Introduction

AC motor drives are broadly used in industry. Induction motors (IMs) and permanent magnet synchronous motors are two types of AC motors that are employed in AC drive systems. Variable frequency control techniques are suggested in numerous industrial applications, which can provide cost-effectiveness and save energy for IMs [1–5]. Direct torque control and field-oriented control (FOC) are two popular control techniques for IMs [6].

In [7–9] it was shown that, with some changes in the conventional control block diagram of the 3-phase IM, vector control of a 3-phase IM during an open-phase fault is possible. In the proposed methods in [7–9] transformation matrices were introduced and applied to the equations of a faulty IM. The aim of using these matrices in [7–9] was to obtain a balanced structure for faulty motor equations. To simplify the vector control equations in [7–9], the backward components of stator voltage equations were neglected. However, neglecting the backward components is reflected in the motor torque and speed oscillations. Furthermore, due to using transformation matrices, the presented techniques in [7–9] are more sensitive to variations of motor parameters, which can be an important issue, especially during open-phase faults.

Several techniques have been introduced for vector control of single-phase IMs or unbalanced 2-phase IMs. Since the structure of a faulty IM is similar to that of a single-phase IM, these control techniques can also be applied to faulty IMs [10–21]. In [10] stator FOC of a single-phase IM with a current double sequence controller

*Correspondence: jmohammad6@live.utm.my

was proposed; the use of the current double sequence controller resulted in a complex control system. In [9,11] rotor FOC (RFOC) of a 2-phase IM with a hysteresis current controller was used, which has a major drawback in light load conditions. In [12], RFOC of a single-phase IM based on a voltage controller was implemented. For high performance vector control of single-phase IMs, vector control of a single-phase IM with estimation of the motor speed based on stator currents [13], extended Kalman filter (EKF) [14], and model reference adaptive system [15,16] have been proposed. The control strategy in [13–17] is based on that of [11]. In most of the previously presented schemes for vector control of 2-phase IMs, the assumption $L_{qs}/L_{ds} = (M_q/M_d)^2$ has been used [11–19] in order to simplify the analysis and control. In [20] the differences in the performance of the drive system with and without the assumption of $L_{qs}/L_{ds} = (M_q/M_d)^2$ were studied. It was shown that low frequency oscillation existed in the torque and the speed responses of the drive system when $L_{qs}/L_{ds} = (M_q/M_d)^2$ was assumed. In [20] a method without considering $L_{qs}/L_{ds} = (M_q/M_d)^2$ for vector control of a 2-phase IM was proposed. However, the performance of the proposed method in [20] is sensitive to the variations of motor parameters. In [21] common problems encountered in the conventional vector control of single-phase IMs were discussed and a RFOC method for a symmetrical 2-phase IM was proposed in that paper. The implementation of FOC for a symmetrical 2-phase IM is simpler than conventional vector control of an asymmetrical single-phase IM. However, this method cannot be used for vector control of faulty IMs because of unequal stator windings in the faulty IM model [7].

One of the best known failures in stator windings of electrical machines is the open circuit. Opening-phase faults occur by the opening of windings, blown fuses, etc. In the literature, several methods based on the EKF, neural networks, fuzzy logic, etc. have been presented to detect stator winding faults in electrical machines [22–29].

The main contribution of this research is the development of a FOC strategy for 3-phase IM drives, which can be used for healthy and faulty 3-phase IMs. Differently from the conventional FOC, the proposed technique uses backward and forward transformation matrices alternately to perform FOC of the IM. In this paper, the BI-FOC (bi-input field-oriented control) method for speed control of a 3-phase IM is simulated using MATLAB and tested under open-phase fault conditions. It should be pointed out that the fault detection in this paper is based on a comparison between real speed and reference speed. A more practical and effective technique of fault detection should be based on [22–29]. It is not the objective of this paper to evaluate fault detection techniques.

This paper is organized as follows: in section 2, the models of 3-phase IMs, 2-phase IMs, and 1-phase IMs are presented. Section 3 introduces the development of the FOC technique for a faulty 3-phase IM. The simulation results and comparisons are presented in Section 4. Section 5 gives the experimental results and the conclusion is presented in Section 6.

2. The d-q model of the IM

The well-known 2-phase model of a 3-phase IM in stationary reference frame (superscript "s") can be expressed by the following equations [6]:

$$v_{ds}^s = r_s i_{ds}^s + \frac{d\lambda_{ds}^s}{dt} \tag{1a}$$

$$v_{qs}^s = r_s i_{qs}^s + \frac{d\lambda_{qs}^s}{dt} \tag{1b}$$

$$\lambda_{ds}^{s} = L_{ds} i_{ds}^{s} + M_{d} i_{dr}^{s} \tag{1c}$$

$$\lambda_{qs}^{s} = L_{qs} i_{qs}^{s} + M_{q} i_{qr}^{s} \tag{1d}$$

$$v_{dr}^{s} = 0 = r_{r} i_{dr}^{s} + \frac{d\lambda_{dr}^{s}}{dt} + \omega_{r} \lambda_{qr}^{s} \tag{1e}$$

$$v_{qr}^{s} = 0 = r_{r} i_{qr}^{s} + \frac{d\lambda_{qr}^{s}}{dt} - \omega_{r} \lambda_{dr}^{s} \tag{1f}$$

$$\lambda_{dr}^{s} = L_{r} i_{dr}^{s} + M_{d} i_{ds}^{s} \tag{1g}$$

$$\lambda_{qr}^{s} = L_{r} i_{qr}^{s} + M_{q} i_{qs}^{s} \tag{1h}$$

Here, for a healthy 3-phase IM [6]:

$$L_{ds} = L_{ls} + \frac{3}{2} L_{ms}, L_{qs} = L_{ls} + \frac{3}{2} L_{ms}, M_{d} = \frac{3}{2} L_{ms}, M_{q} = \frac{3}{2} L_{ms}, L_{r} = L_{lr} + \frac{3}{2} L_{ms} \tag{1i}$$

In the faulty mode (one-phase cut-off) [7,30]:

$$L_{ds} = L_{ls} + \frac{3}{2} L_{ms}, L_{qs} = L_{ls} + \frac{1}{2} L_{ms}, M_{d} = \frac{3}{2} L_{ms}, M_{q} = \frac{\sqrt{3}}{2} L_{ms}, L_{r} = L_{lr} + \frac{3}{2} L_{ms} \tag{1j}$$

In the faulty mode (two-phase cut-off) [31]:

$$L_{ds} = L_{ls} + L_{ms}, L_{qs} = 0, M_{d} = \sqrt{\frac{3}{2}} L_{ms}, M_{q} = 0, L_{r} = L_{lr} + \frac{3}{2} L_{ms} \tag{1k}$$

As can be seen from Eqs. (1a)–(1h), the faulty 3-phase IM equations are similar to the balanced 3-phase IM equations. In fact, by changing the motor parameters in Eqs. (1a)–(1h), we can obtain the equations of balanced and faulty 3-phase IMs.

Electromagnetic torque and motion equations can be written as [7,30]:

$$\tau_{e} = \frac{P}{2} (M_{q} i_{qs}^{s} i_{dr}^{s} - M_{d} i_{ds}^{s} i_{qr}^{s}) \tag{2a}$$

$$\frac{P}{2} (\tau_{e} - \tau_{l}) = J \frac{d\omega_{r}}{dt} + F \omega_{r} \tag{2b}$$

Using the following substitutions:

$$v_{ds}^{s} = v_{x_1 s}^{s} + j v_{y_1 s}^{s} \tag{3a}$$

$$i_{ds}^{s} = i_{x_1 s}^{s} + j i_{y_1 s}^{s} \tag{3b}$$

$$v_{dr}^{s} = v_{x_1 r}^{s} + j v_{y_1 r}^{s} \tag{3c}$$

$$i^s_{dr} = i^s_{x_1r} + ji^s_{y_1r} \tag{3d}$$

$$\lambda^s_{qr} = \lambda^s_{x_2r} + j\lambda^s_{y_2r} \tag{3e}$$

Eqs. (1a)–(1h) can be modified as Eqs (4a)–(5b):

$$v^s_{x_1s} = r_s i^s_{x_1s} + L_{ls}\frac{di^s_{x_1s}}{dt} + M_d\left(\frac{di^s_{x_1s}}{dt} + \frac{di^s_{y_1r}}{dt}\right) \tag{4a}$$

$$v^s_{y_1s} = r_s i^s_{y_1s} + L_{ls}\frac{di^s_{y_1s}}{dt} + M_d\left(\frac{di^s_{y_1s}}{dt} + \frac{di^s_{x_1r}}{dt}\right) \tag{4b}$$

$$v^s_{x_1r} = r_r i^s_{x_1r} + L_{lr}\frac{di^s_{x_1r}}{dt} + \omega_r\lambda^s_{x_2r} + M_d\left(\frac{di^s_{x_1r}}{dt} + \frac{di^s_{y_1s}}{dt}\right) \tag{5a}$$

$$v^s_{y_1r} = r_r i^s_{y_1r} + L_{lr}\frac{di^s_{y_1r}}{dt} + \omega_r\lambda^s_{y_2r} + M_d\left(\frac{di^s_{y_1r}}{dt} + \frac{di^s_{x_1s}}{dt}\right) \tag{5b}$$

Based on Eqs. (4a)–(5b), the d-axis equivalent circuit of the faulty IM can be shown as in Figure 1.

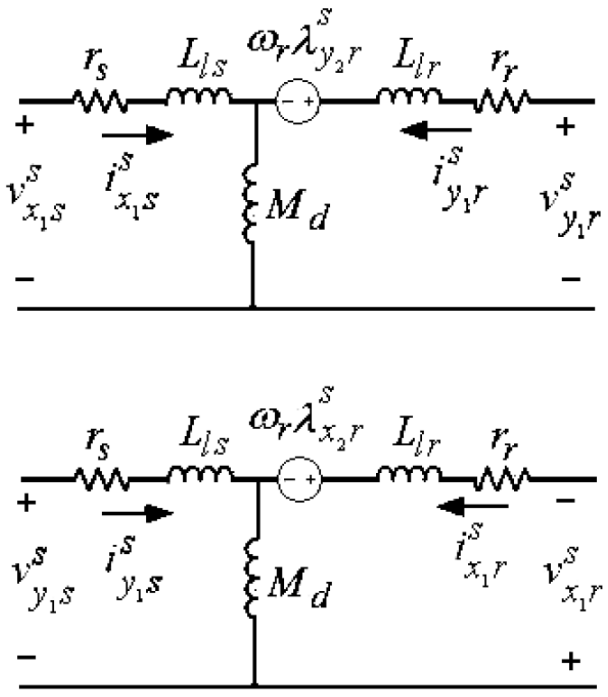

Figure 1. Positive sequence equivalent circuit of IM (d-axis).

Moreover, using substitutions in Eqs. (6a)–(6e), Eqs. (1a)–(1h) can also be modified as in Eqs. (7a)–(8b):

$$v^s_{qs} = v^s_{x_2s} + jv^s_{y_2s} \tag{6a}$$

$$i^s_{qs} = i^s_{x_2s} + ji^s_{y_2s} \tag{6b}$$

$$v^s_{qr} = v^s_{x_2r} + jv^s_{y_2r} \tag{6c}$$

$$i^s_{qr} = i^s_{x_2r} + ji^s_{y_2r} \tag{6d}$$

$$\lambda^s_{dr} = \lambda^s_{x_1r} + j\lambda^s_{y_1r} \tag{6e}$$

$$v^s_{x_2s} = r_s i^s_{x_2s} + L_{ls}\frac{di^s_{x_2s}}{dt} + M_q\left(\frac{di^s_{x_2s}}{dt} + \frac{di^s_{y_2r}}{dt}\right) \tag{7a}$$

$$v^s_{y_2s} = r_s i^s_{y_2s} + L_{ls}\frac{di^s_{y_2s}}{dt} + M_q\left(\frac{di^s_{y_2s}}{dt} + \frac{di^s_{x_2r}}{dt}\right) \tag{7b}$$

$$v^s_{x_2r} = r_r i^s_{x_2r} + L_{lr}\frac{di^s_{x_2r}}{dt} - \omega_r\lambda^s_{x_1r} + M_q\left(\frac{di^s_{x_2r}}{dt} + \frac{di^s_{y_2s}}{dt}\right) \tag{8a}$$

$$v^s_{y_2r} = r_r i^s_{y_2r} + L_{lr}\frac{di^s_{y_2r}}{dt} - \omega_r\lambda^s_{y_1r} + M_q\left(\frac{di^s_{y_2r}}{dt} + \frac{di^s_{x_2s}}{dt}\right) \tag{8b}$$

Based on Eqs. (7a)–(8b), the q-axis equivalent circuit of the faulty IM can be shown as in Figure 2. It can be noted that v^s_{ds}, v^s_{qs}, i^s_{ds}, and i^s_{qs} are the unbalanced voltages and currents of the motor and $v^s_{x_1s}$, $v^s_{x_2s}$, $i^s_{x_1s}$, $i^s_{x_2s}$, $v^s_{y_1s}$, $v^s_{y_2s}$, $i^s_{y_1s}$, $i^s_{y_2s}$ represent balanced voltages and currents of the motor.

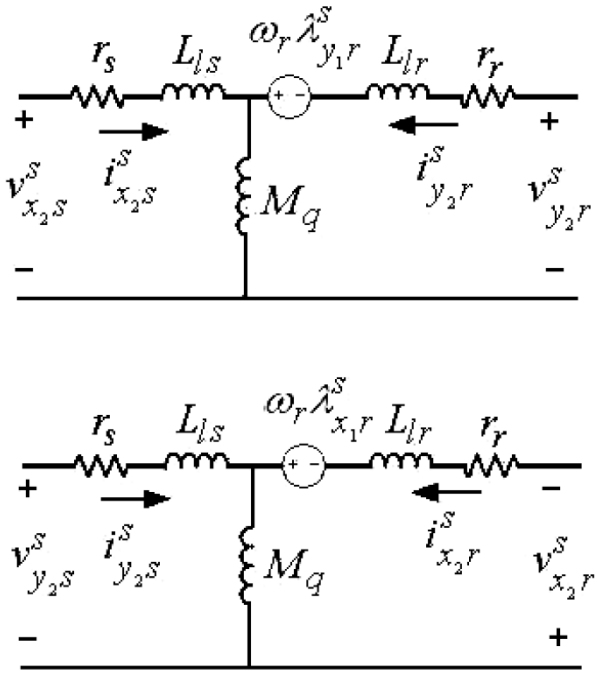

Figure 2. Negative sequence equivalent circuit of IM (q-axis).

As can be seen from Figures 1 and 2, using the proposed change of variables presented in Eqs. (3a)–(3e) and (6a)–(6e), the unbalanced equivalent circuit of the faulty 3-phase IM splits into two balanced circuits. It is expected that by applying Eqs. (3a)–(3e) and (6a)–(6e) to the unbalanced equations of the faulty 3-phase IM, the equations of the faulty motor change into two balanced equations. Using this idea, a modified vector control technique for 3-phase IMs in normal and faulty conditions is proposed.

3. Proposed algorithm for 3-phase IM

In this section, a modified vector control technique is developed for controlling the IM under open-phase faults. Based on Appendix A, from Eqs. (3a)–(3e) we can write the following equation:

$$\begin{bmatrix} F^e_{ds} \\ F^e_{qs} \end{bmatrix} = \underbrace{\begin{bmatrix} \cos\theta_e & \sin\theta_e \\ -\sin\theta_e & \cos\theta_e \end{bmatrix}}_{[T^e_s]} \begin{bmatrix} F^s_{ds} \\ F^s_{qs} \end{bmatrix} \tag{9}$$

In this paper the superscript and subscript "e" denotes that the variables are in the rotating reference frame. Eq. (9) indicates a transformation matrix for the changing of the variables from unbalanced mode to balanced mode. It can be shown that using Eq. (9), the IM equations (Eqs. (1a)–(1h)) are transformed into two balanced equations. By applying Eq. (9) to the IM equations, we have the following:

Stator voltage equations:

$$\begin{aligned} [T^e_s] \begin{bmatrix} v^s_{ds} \\ v^s_{qs} \end{bmatrix} &= [T^e_s] \begin{bmatrix} r_s + L_{ds}\frac{d}{dt} & 0 \\ 0 & r_s + L_{qs}\frac{d}{dt} \end{bmatrix} [T^e_s]^{-1} [T^e_s] \begin{bmatrix} i^s_{ds} \\ i^s_{qs} \end{bmatrix} \\ &\quad + [T^e_s] \begin{bmatrix} M_d\frac{d}{dt} & 0 \\ 0 & M_q\frac{d}{dt} \end{bmatrix} [T^e_s]^{-1} [T^e_s] \begin{bmatrix} i^s_{dr} \\ i^s_{qr} \end{bmatrix} \end{aligned} \tag{10}$$

Rotor voltage equations:

$$\begin{aligned} [T^e_s] \begin{bmatrix} 0 \\ 0 \end{bmatrix} &= [T^e_s] \begin{bmatrix} M_d\frac{d}{dt} & \omega_r M_q \\ -\omega_r M_d & M_q\frac{d}{dt} \end{bmatrix} [T^e_s]^{-1} [T^e_s] \begin{bmatrix} i^s_{ds} \\ i^s_{qs} \end{bmatrix} \\ &\quad + [T^e_s] \begin{bmatrix} r_r + L_r\frac{d}{dt} & \omega_r L_r \\ -\omega_r L_r & r_r + L_r\frac{d}{dt} \end{bmatrix} [T^e_s]^{-1} [T^e_s] \begin{bmatrix} i^s_{dr} \\ i^s_{qr} \end{bmatrix} \end{aligned} \tag{11}$$

In these equations $[T^e_s]$ is defined as in Eq. (9). After simplification, Eqs. (10) and (11) can be written as Eqs.

(12a) and (12b):

$$\begin{bmatrix} v_{ds}^{e} \\ v_{qs}^{e} \\ 0 \\ 0 \end{bmatrix} = \begin{bmatrix} r_s + (\frac{L_{ds}+L_{qs}}{2})\frac{d}{dt} & -\omega_e(\frac{L_{ds}+L_{qs}}{2}) & (\frac{M_d+M_q}{2})\frac{d}{dt} & -\omega_e(\frac{M_d+M_q}{2}) \\ \omega_e(\frac{L_{ds}+L_{qs}}{2}) & r_s + (\frac{L_{ds}+L_{qs}}{2})\frac{d}{dt} & \omega_e(\frac{M_d+M_q}{2}) & (\frac{M_d+M_q}{2})\frac{d}{dt} \\ (\frac{M_d+M_q}{2})\frac{d}{dt} & -(\omega_e-\omega_r)(\frac{M_d+M_q}{2}) & r_r + L_r\frac{d}{dt} & -(\omega_e-\omega_r)L_r \\ (\omega_e-\omega_r)(\frac{M_d+M_q}{2}) & (\frac{M_d+M_q}{2})\frac{d}{dt} & (\omega_e-\omega_r)L_r & r_r + L_r\frac{d}{dt} \end{bmatrix} \begin{bmatrix} i_{ds}^{+e} \\ i_{qs}^{+e} \\ i_{dr}^{+e} \\ i_{qr}^{+e} \end{bmatrix}$$

$$+ \begin{bmatrix} (\frac{L_{ds}-L_{qs}}{2})\frac{d}{dt} & \omega_e(\frac{L_{ds}-L_{qs}}{2}) & (\frac{M_d-M_q}{2})\frac{d}{dt} & \omega_e(\frac{M_d-M_q}{2}) \\ \omega_e(\frac{L_{ds}-L_{qs}}{2}) & -(\frac{L_{ds}-L_{qs}}{2})\frac{d}{dt} & \omega_e(\frac{M_d-M_q}{2}) & -(\frac{M_d-M_q}{2})\frac{d}{dt} \\ (\frac{M_d-M_q}{2})\frac{d}{dt} & (\omega_e-\omega_r)(\frac{M_d+M_q}{2}) & 0 & 0 \\ (\omega_e-\omega_r)(\frac{M_d-M_q}{2}) & -(\frac{M_d-M_q}{2})\frac{d}{dt} & 0 & 0 \end{bmatrix} \begin{bmatrix} i_{ds}^{-e} \\ i_{qs}^{-e} \\ i_{dr}^{-e} \\ i_{qr}^{-e} \end{bmatrix} \tag{12a}$$

where,

$$\begin{bmatrix} i_{ds}^{+e} \\ i_{qs}^{+e} \end{bmatrix} = \begin{bmatrix} \cos\theta_e & \sin\theta_e \\ -\sin\theta_e & \cos\theta_e \end{bmatrix} \begin{bmatrix} i_{ds}^{s} \\ i_{qs}^{s} \end{bmatrix}, \quad \begin{bmatrix} i_{dr}^{+e} \\ i_{qr}^{+e} \end{bmatrix} = \begin{bmatrix} \cos\theta_e & \sin\theta_e \\ -\sin\theta_e & \cos\theta_e \end{bmatrix} \begin{bmatrix} i_{dr}^{s} \\ i_{qr}^{s} \end{bmatrix}$$

$$\begin{bmatrix} i_{ds}^{-e} \\ i_{qs}^{-e} \end{bmatrix} = \begin{bmatrix} \cos\theta_e & -\sin\theta_e \\ \sin\theta_e & \cos\theta_e \end{bmatrix} \begin{bmatrix} i_{ds}^{s} \\ i_{qs}^{s} \end{bmatrix}, \quad \begin{bmatrix} i_{dr}^{-e} \\ i_{qr}^{-e} \end{bmatrix} = \begin{bmatrix} \cos\theta_e & -\sin\theta_e \\ \sin\theta_e & \cos\theta_e \end{bmatrix} \begin{bmatrix} i_{dr}^{s} \\ i_{qr}^{s} \end{bmatrix} \tag{12b}$$

In general, Eq. (12a) is composed of two groups of equations: equations with superscript $+e$ representing the forward components, and equations with superscript $-e$ representing the backward components. The terms with superscript $-e$, which is the backward component of the IM equations, exist because of the unequal inductances in Eq. (1a). The d-q axis representing these two groups of equations is graphically depicted in Figure 3. It can be noted that, in the healthy 3-phase IM equations, there are no backward components. These terms cause oscillations in the machine torque during open-phase faults.

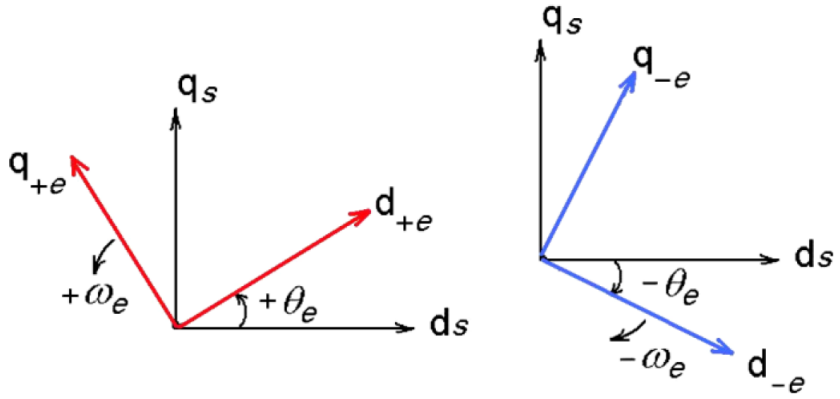

Figure 3. Forward, backward, and stationary frame (forward: subscript + e, backward: subscript - e, stationary: subscript s).

As can be seen from Eq. (12a), the structure of the forward or backward terms is similar to the conventional FOC equations of a balanced 3-phase IM. The conventional FOC of a balanced 3-phase IM is fully discussed in Appendix B. The only difference between the equations for the forward components of Eq. (12a) and the balanced 3-phase IM equations is that, in the forward components of Eq. (12a), $M=(M_d+M_q)/2$ and $L_s=(L_{ds}+L_{qs})/2$, whereas in the balanced IM we have $M=3/2\ L_{ms}$ and $L_s=L_{ls}+3/2\ L_{ms}$. On the other hand, the difference between the equation of the backward components of Eq. (12a) and the balanced 3-phase IM equations is that, in the backward components of Eq. (12a) $r_s=0$, $r_r=0$, $L_r=0$, $M=(M_d-M_q)/2$, $L_s=(L_{ds}-L_{qs})/2$, and a negative value of i^e_{qs} and i^e_{qr}, but in the balanced IM we have r_s, r_r, L_r, M, L_s, and positive values of i^e_{qs} and i^e_{qr}. Therefore, two conventional FOCs to control the forward and backward components can be utilized for vector control of both healthy and faulty 3-phase IMs, as shown in Figure 4. It can be noted that the structures of FOC-Forward and FOC-Backward in Figure 4 are similar to the conventional FOC algorithm. The difference between FOC-Forward and FOC-Backward with conventional FOC is the same as the difference between equations of the forward and backward components with the equations of the balanced 3-phase IM, which have been discussed before. In Figure 4, in order to alternately switch between the two states, two switches are employed whereby the switches will alternately change positions at each sampling time. It should be noted that in both normal and faulty conditions, these switches are consecutively changed at each time step and depending on IM conditions (healthy mode or faulty mode), only motor parameters are changed. On the other hand, there are both forward and backward components during normal and open-phase fault conditions. As can be seen from Figure 4, in the normal condition, due to the equal machine inductances, the backward components of Eq. (12a) and therefore FOC-Backward are removed.

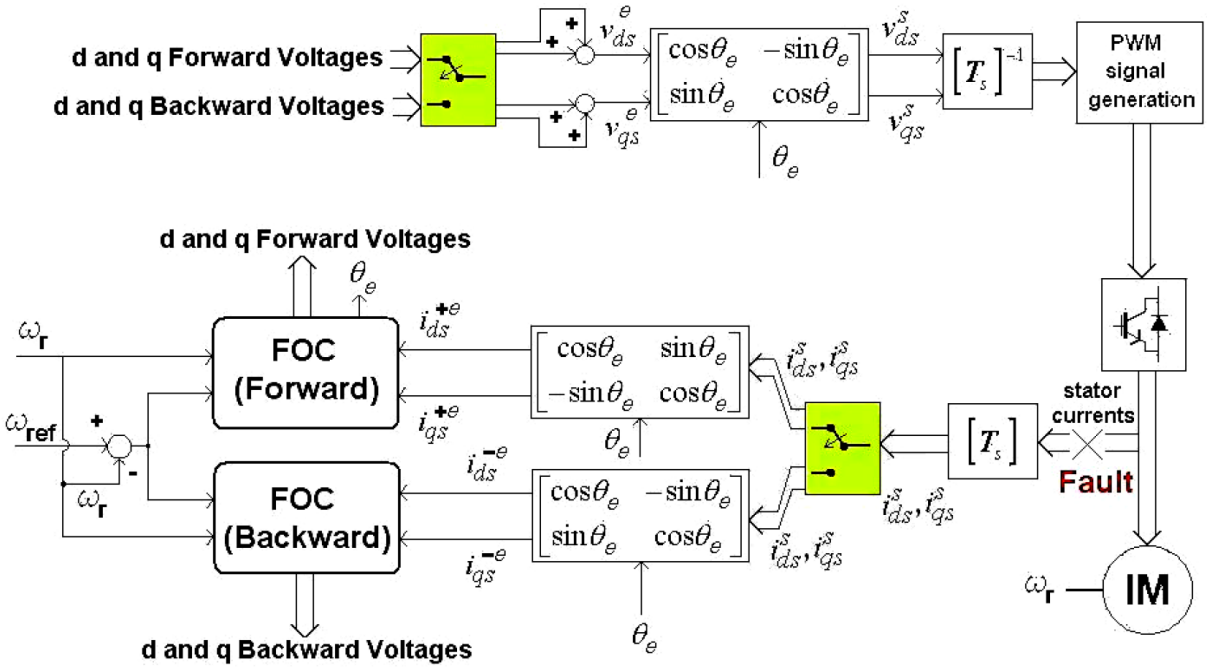

Figure 4. Block diagram of proposed method for vector control of both healthy and faulty 3-phase IMs using forward and backward components.

As a result, to simplify Figure 4, a single FOC algorithm with the alternate sampling and execution of two different stator currents (i^{+e} and i^{-e}) can be used for vector control of balanced and faulty 3-phase IMs. The

block diagram of the modified FOC of the 3-phase IM technique is shown in Figure 5. The proposed technique essentially consists of a conventional indirect FOC with the use of backward and forward transformation matrices. This scheme can be used for a 3-phase IM under normal conditions, one-phase cut-off fault, and two-phase cut-off fault by switching the motor parameters as shown in Eqs. (1i), (1j), and (1k) respectively.

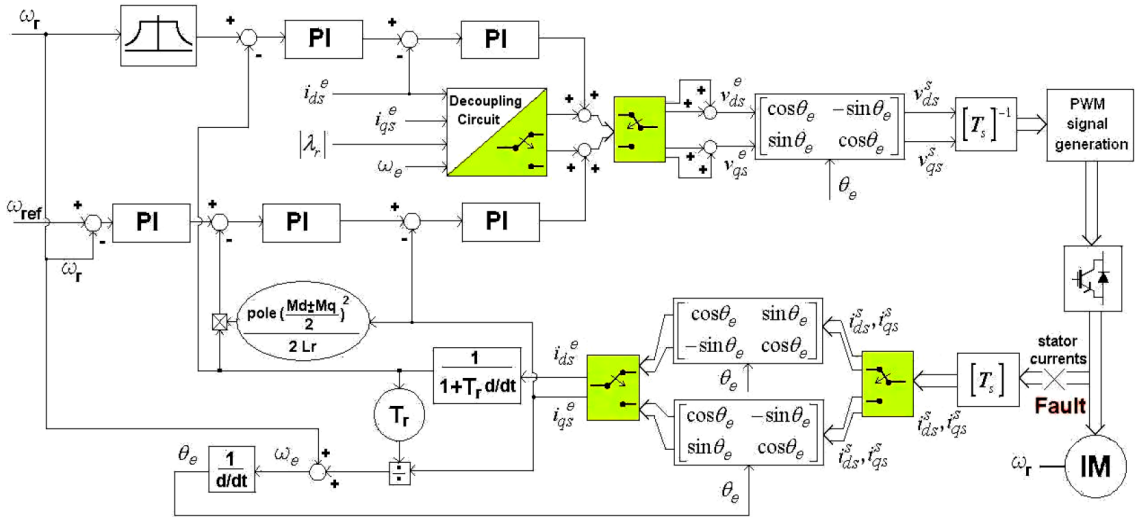

Figure 5. Block diagram of BI-RFOC.

In this paper, a method for vector control of 3-phase IMs under an open-phase fault has been proposed with some changes to the conventional FOC technique. These changes are transformation matrices, motor parameters, and PI controller coefficients. It should be pointed out that PI controller coefficients affect the accuracy of the proposed method. In this paper, the PI controllers during normal and faulty conditions are optimized using a trial-and-error process.

4. Simulation results and comparisons

In order to study the effectiveness of the proposed BI-RFOC, simulations for a 3-phase IM drive system with and without BI-RFOC are performed under normal and open-phase fault conditions. Simulations are performed using MATLAB software. The Runge–Kutta 4th order method is used for solving dynamic equations of balanced and faulty IMs. In the simulations, the reference speed is set to 55 rad/s. Moreover, as mentioned before in this paper, very fast fault detection is assumed. In other words, from t = 0 s to t = t_{fault} s, the IM runs in healthy mode and the motor is modeled using healthy 3-phase IM equations. At t = t_{fault} s, a fault is introduced and hence for t $\geq$ t_{fault} s the IM is simulated using the faulty machine equations as given by Eq. (1j). The ratings and parameters of the 3-phase IM are as given in Appendix C.

Figure 6 illustrates the results of the conventional controller that is used for healthy and faulty conditions. Figure 6a shows the stator a-axis current, Figure 6b shows torque, and Figure 6c shows speed. Moreover, Figure 7 shows the simulation results of BI-FOC for vector control of the 3-phase IM under healthy and faulty conditions. Figure 7a shows the stator a-axis current, Figure 7b shows torque, and Figure 7c shows speed. In both figures, the IM is started with balanced condition and then a phase cut-off fault happens in phase "C" and at t = 2 s.

The results in Figures 6 and 7 show that the conventional controller is unable to control the unbalanced 3-phase IM precisely after the fault is introduced. It can be seen that the proposed controller produces less

speed and torque ripple compared to the conventional FOC. As can be seen from Figures 6b and 7b, by using a conventional controller, the torque peak-peak oscillation at steady state is $\sim$4 Nm, but using the proposed controller the torque peak-peak oscillation at steady-state is $\sim$2 Nm. From these figures, it can be concluded that the performance of the modified control system for a faulty motor is better than the conventional control system in terms of decreasing the motor speed and torque oscillations.

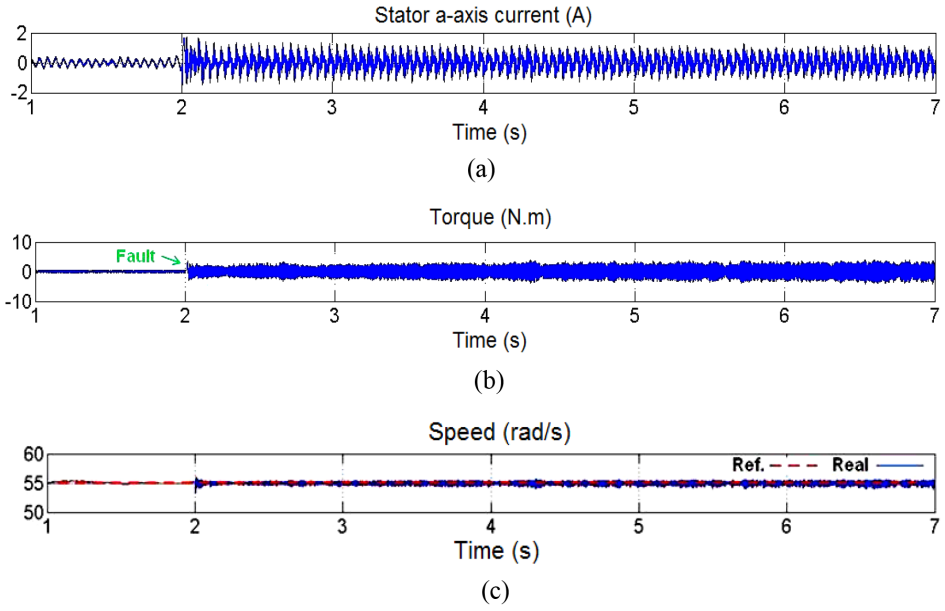

Figure 6. Simulation results of the conventional FOC for healthy and faulty 3-phase IMs: a) stator a-axis current, b) torque, c) speed.

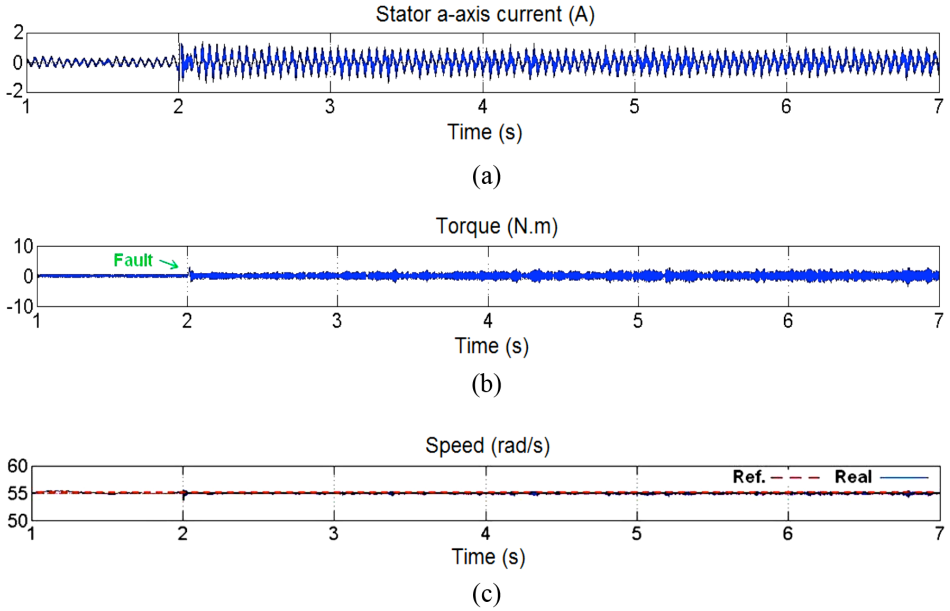

Figure 7. Simulation results of the BI-FOC for healthy and faulty 3-phase IMs: a) stator a-axis current, b) torque, c) speed.

5. Experimental results

In Section 4, simulation tests of the conventional and proposed methods were carried out. The objective of carrying out the simulations in Section 4 was to verify the effectiveness of the proposed method for a faulty 3-phase IM and at the same time to compare their performances with the conventional method. In Section 4, the parameters of the IM used in the simulations are ideal assuming that the parameters of the motor completely match the parameters used in the controllers. In this section, experimental results of the healthy and faulty 3-phase IMs based on conventional and proposed methods are presented.

A photograph of the experimental set-up test is shown in Figure 8, where the star connected 3-phase IM is supplied by a 3-leg VSI built using 3 IGBT modules. An incremental encoder and two Hall effect current sensors to measure machine speed and stator currents are used. An electronic switch is connected in series to phase "C" of the stator winding and is activated to open this phase during the motor operation. The experimentation is carried out using MATLAB/Simulink software and the dSPACE DS1104 real-time R&D controller board. A real-time interface is used to link between the dSPACE real-time R&D controller board and the MATLAB

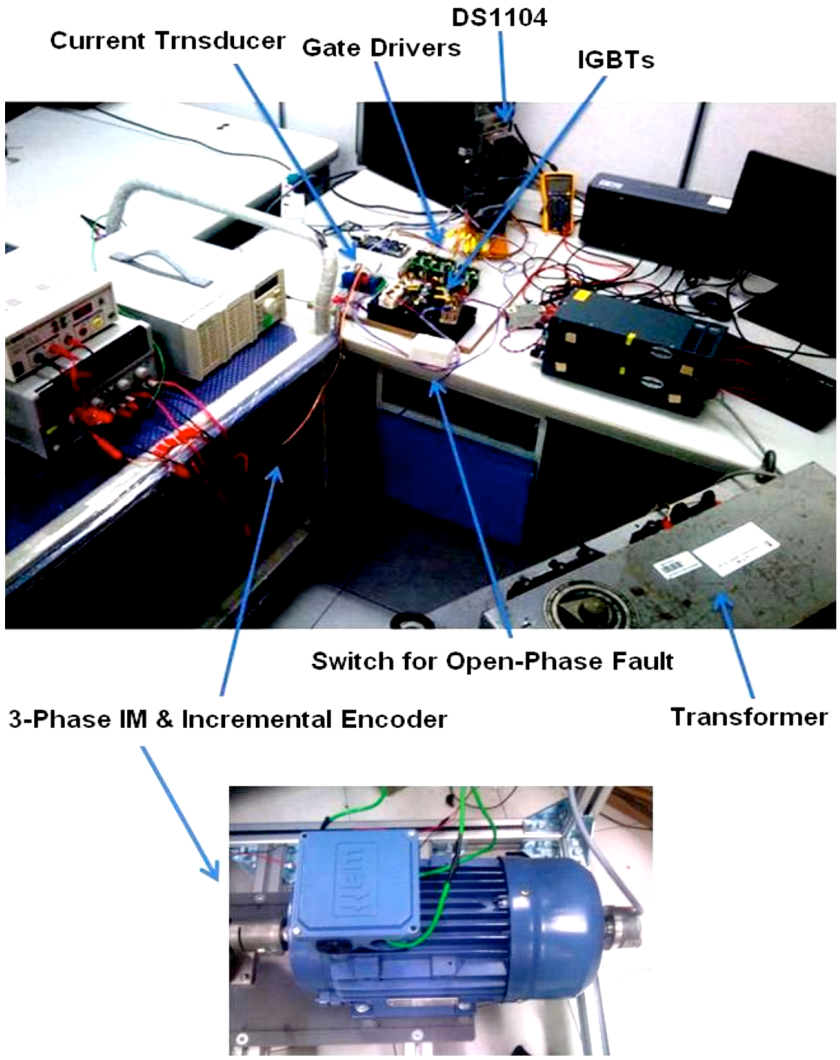

Figure 8. Photograph of the experimental test system.

software. A PWM technique with dead time of 2 μs is used for the 3-leg inverter. The sampling time of the implemented control algorithm is fixed to 250 μs. The parameters of the 3-phase IM are given in Appendix C. It should be noted that during open-phase fault conditions, the currents in the remaining active stator phases are dependent on each other and cannot be controlled separately. To overcome this problem, the neutral point of the 3-phase IM should be accessible and connected to the midpoint of the DC bus of the drive system. In the experiments, the neutral point of the 3-phase IM is connected to the midpoint of the DC bus.

To confirm the effectiveness of the proposed control strategy, three tests were performed. In the first test (blue color in Figure 9; Figure 9a: speed response, Figure 9b: torque response), the 3-phase IM started under normal conditions and then a phase cut-off was applied at 22.4 s. In the second test (red color in Figure 9), the 3-phase IM started under normal conditions and then a phase cut-off was applied at 23.5 s. In the first test, the conventional controller is used and in the second test the proposed controller is applied. Throughout the experiments, the torque during the healthy and faulty conditions is estimated based on equations of the machine;

$$\tau_e = \frac{P}{2} \times \frac{M_d \pm M_q}{2L_r} \times |\lambda_r| \times i_{qs}^e.$$

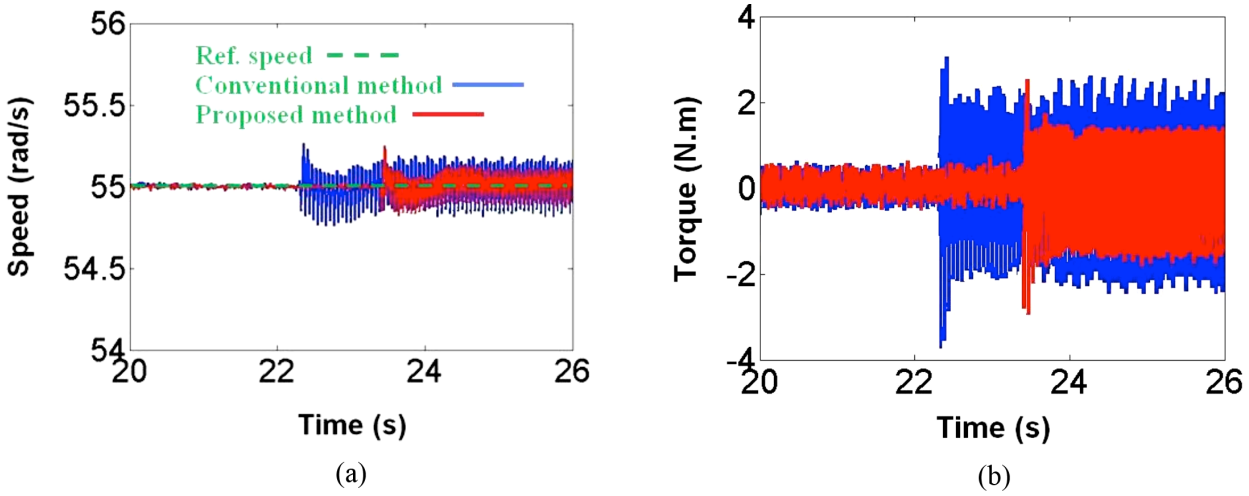

Figure 9. Experimental results of the conventional and proposed methods for healthy and faulty 3-phase IMs: a) speed, b) torque.

Comparison of the performance between the proposed controller and the conventional controller can be clearly seen in Figure 9. It can be seen that the proposed drive system performs good speed tracking even during stator winding open-phase faults. Moreover, a significant reduction in the motor speed and torque oscillations can be observed when the proposed strategy is activated. It can be observed that the proposed strategy is able to minimize the motor speed and torque pulsations. It should be noted that although conventional and proposed techniques were able to control the 3-phase machine under open-phase faults, in general, the proposed method provides better steady-state performance, especially in decreasing motor speed and torque pulsations. A summary of the comparison between experimental results of the conventional and proposed methods in terms of steady-state speed and torque responses is presented in the Table.

To verify the effectiveness of the proposed drive system, two different tests are performed. In these tests, the drive system is started under normal conditions and later an open-phase fault is applied in phase "C" of the stator windings. Figure 10 shows the experimental results of the comparison between stator currents after the open-phase fault. Figure 10a shows the waveform of faulty IM stator a-axis current while the fault-tolerant

Table. Comparison between experimental results of the conventional and proposed methods in terms of steady-state speed and torque responses.

	Conventional method	Proposed method
Speed peak-peak oscillation	0.35 rad/s	0.2 rad/s
Torque peak-peak oscillation	5 Nm	3 Nm

control strategy was deactivated. Figure 10b shows the waveform of faulty IM stator a-axis current when the proposed fault-tolerant control strategy was activated. Figure 10c shows the waveform of faulty IM stator b-axis current while the fault-tolerant control strategy was deactivated and Figure 10d shows the waveform of faulty IM stator b-axis current when the proposed fault-tolerant control strategy was activated. In both tests, the reference speed is set to 65 rad/s. It is seen from Figure 10 that the sinusoidal form of the stator currents is maintained at the rotor speed of 65 rad/s when the introduced drive system is activated.

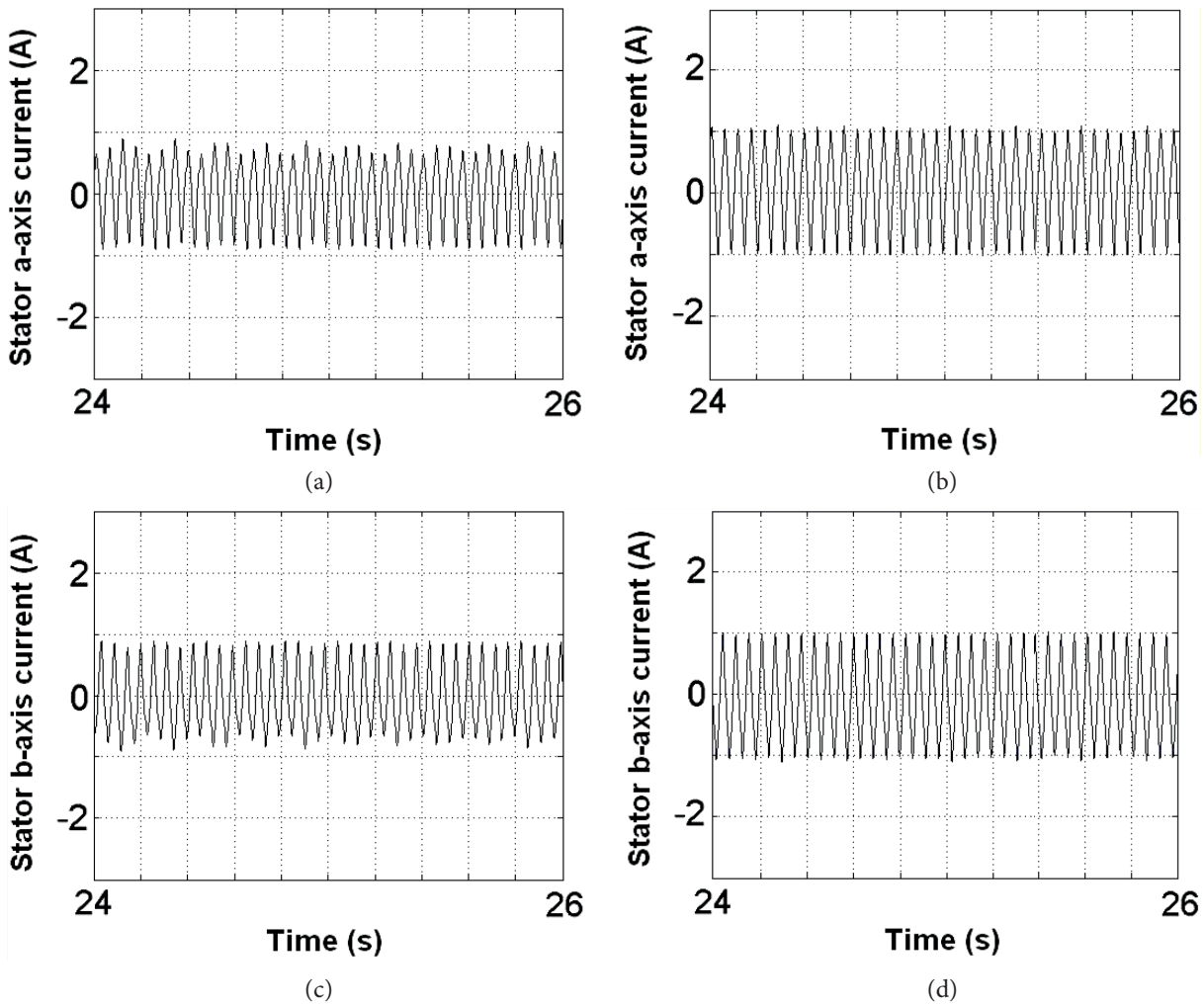

Figure 10. Experimental results of the conventional and proposed methods for faulty 3-phase IM: a) stator a-axis current- conventional, b) stator a-axis current- proposed c) stator b-axis current- conventional, d) stator b-axis current- proposed.

To confirm the effectiveness of the proposed strategy, two different tests were performed. Figures 11a and 11b show the waveform of faulty IM speed using the conventional and proposed methods, respectively. Moreover, Figures 11c and 11d show the waveform of faulty IM torque using the conventional and proposed strategies. As shown in Figure 11, the proposed algorithm exhibits good tracking error performances and faster response when compared to the conventional method. It can be seen that the time to reach the steady state is shorter with the proposed controller. From Figure 11, a reduction in the motor speed and torque oscillations can be observed when the proposed strategy is used.

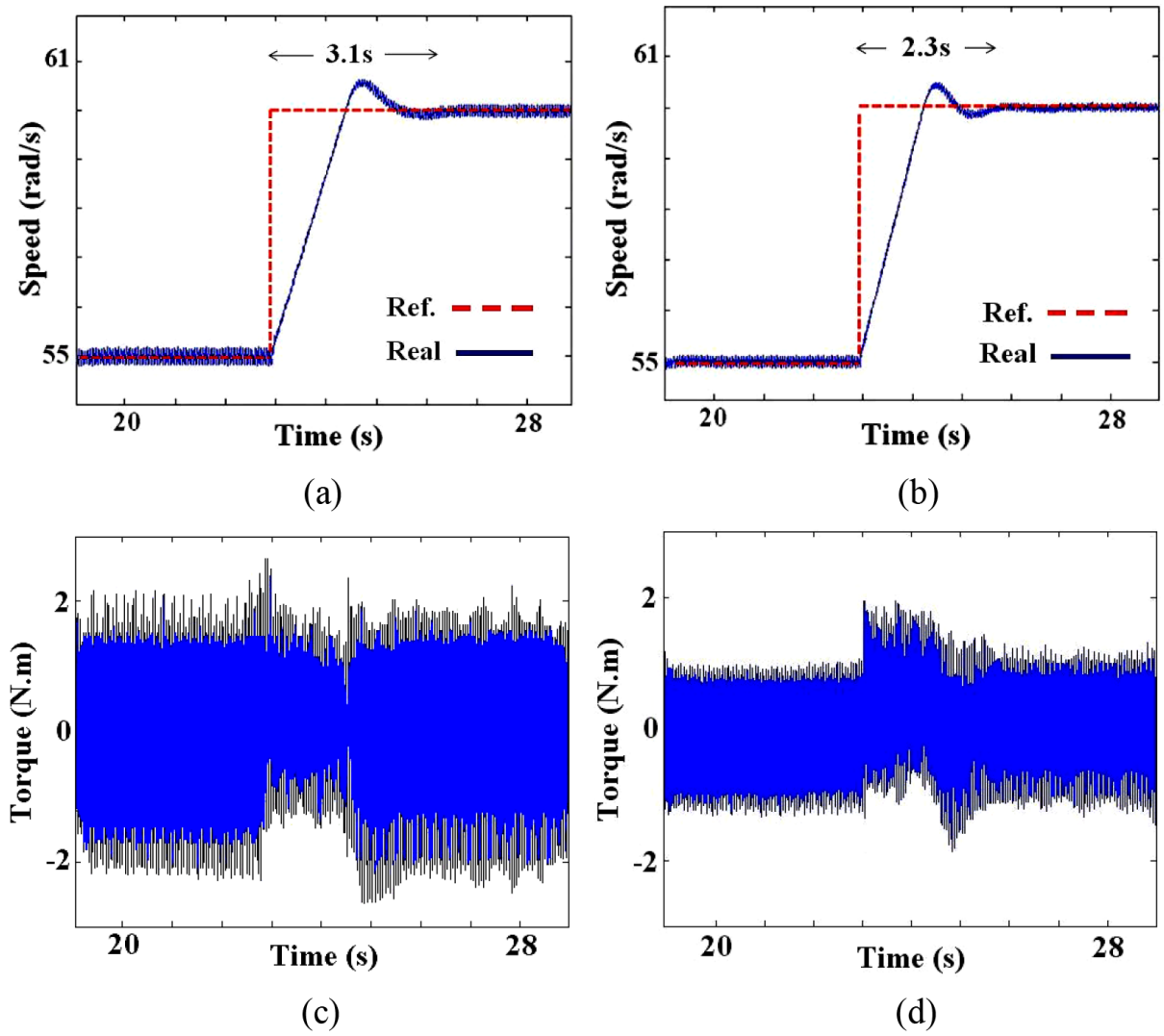

Figure 11. Experimental results of the conventional and proposed methods for faulty 3-phase IM: a) speed- conventional, b) speed- proposed, c) torque- conventional, d) torque- proposed.

In this paper, the results obtained from the experiments show the effect of the proposed control topology in decreasing the speed and torque pulsations under open-phase fault of a star-connected 3-phase motor drive (see Figure 9), its effect in decreasing the unbalances in the motor stator currents (see Figure 10), and the effect of the proposed control system in decreasing the time to reach the steady state (see Figure 11).

6. Conclusion

In this study, a modified FOC of a 3-phase IM, named BI-FOC, has been introduced that enables the control of a 3-phase IM under open-phase fault conditions. The control principle is developed based on the modeling of the unbalanced 3-phase IM using the forward and backward components. Based on simulation and experimental results, the BI-FOC method has managed to significantly reduce the oscillation in the torque and speed responses under open-circuit fault. The proposed method in this paper not only can be used for critical industrial applications where we need to have a fault-tolerant drive system but also can be used for vector control of single-phase IMs and faulty single-phase IMs with unequal auxiliary and main windings.

Nomenclature

v^s_{ds}, v^s_{qs}	Stator d-q axes voltages
$i^s_{ds}, i^s_{qs}, i^s_{dr}, i^s_{qr}$	Stator and rotor d-q axes currents
$\lambda^s_{ds}, \lambda^s_{qs}, \lambda^s_{dr}, \lambda^s_{qr}$	Stator and rotor d-q axes fluxes
r_s , r_r	Stator and rotor resistances
M_d , M_q	d-q axes mutual inductances
M	Mutual inductance
L_{ds} , L_{qs}	d-q axes stator self-inductances
L_s, L_r	Stator and rotor self-inductances
L_{ls} , L_{lr}	Stator and rotor leakage inductances
L_{ms}	Magnetizing inductance
ω_e	Rotor angular speed
θ_e	Angle between the stationary reference frame and the rotating reference frame
T_r	Rotor time constant
ω_r	Motor's electrical speed
τ_e, τ_l	Electromagnetic torque and load torque
P	Number of poles
J	Moment of inertia
F	Viscous friction coefficient

References

[1] Belkacem S, Naceri F, Abdessemed R. Reduction of torque ripple in DTC for induction motor using input-output feedback linearization. Turk J Electr Eng Co 2012; 20: 273-285.

[2] Saidur R, Mekhilef S, Ali MB, Safari A, Mohammed HA. Applications of variable speed drive (VSD) in electrical motors energy savings. Renew Sust Energ Rev 2012; 16: 543-550.

[3] Zahedi B, Vaez-Zadeh S. Efficiency optimization control of single-phase induction motor drives. IEEE T Power Electr 2009; 24: 1062-1070.

[4] Ilango GS, Rajasekar N. An improved energy saving v/f control technique for solar powered single-phase induction Motor. Energ Convers Manage 2009; 50: 2913-2918.

[5] Davari SA, Khaburi DA, Wang F, Kennel R. Robust sensorless predictive control of induction motors with sliding mode voltage model observer. Turk J Electr Eng Co 2013; 21: 1539-1552.

[6] Vas P. Vector Control of AC Machines. Oxford, UK: Oxford University Press, 1990.

[7] Jannati M, Idris NRN, Salam Z. A new method for modeling and vector control of unbalanced induction motors. In: IEEE 2012 Energy Conversion Congress and Exposition; 15–20 September 2012; Raleigh, NC, USA. New York, NY, USA: IEEE. pp. 3625-3632.

[8] Jannati M, Fallah E. Modeling and vector control of unbalanced induction motors (faulty three phase or single phase induction motors). In: IEEE 2010 1st Conference on Power Electronic & Drive Systems & Technologies; 17–18 February 2010; Tehran, Iran. New York, NY, USA: IEEE. pp. 208-211.

[9] Jannati M, Monadi A, Idris NRN, Aziz MJA, Faudzi AAM. Vector control of faulty three-phase induction motor with an adaptive sliding mode control. Prz Elektrotechniczn 2013; 89: 116-120.

[10] Beltrao de Rossiter Correa M, Jacobina CB, Cabral da Silva ER, Lima AMN. Vector control strategies for single-phase induction motor drive systems. IEEE T Ind Electron 2004; 51: 1073-1080.

[11] de Rossiter Corrêa MB, Jacobina CB, Lima AMN, da Silva ERC. Rotor-flux-oriented control of a single-phase induction motor drive. IEEE T Ind Electron 2000; 47: 832-841.

[12] Jemli M, Azza HB, Gossa M. Real-time implementation of IRFOC for single-phase induction motor drive using dSpace DS 1104 control board. Simul Model Pract Th 2009; 17: 1071-1080.

[13] Jemli M, Ben Azza H, Boussak M, Gossa M. Sensorless indirect stator field orientation speed control for single-phase induction motor drive. IEEE T Power Electr 2009; 24: 1617-1627.

[14] Jannati M, Fallah E. A new method for speed sensorless vector control of single-phase induction motor using extended Kalman filter. In: IEEE 2011 19th Iranian Conference on Electrical Engineering; 17–19 May 2010; Tehran, Iran. New York, NY, USA: IEEE. pp. 1-5.

[15] Azza HB, Jemli M, Boussak M, Goss M. Implementation of sensorless speed control for two-phase induction motor drive using ISFOC strategy. Iran J Sci Technol B 2011; 35: 63-74.

[16] Vieira RP, Grundling HA. Sensorless speed control with a MRAS speed estimator for single-phase induction motors drives. In: IEEE 2009 13th European Conference on Power Electronics and Applications; 8–10 September 2009; Barcelona, Spain. New York, NY, USA: IEEE. pp. 1-10.

[17] Azza HB, Jemli M, Boussak M, Gossa M. High performance sensorless speed vector control of SPIM drives with on-line stator resistance estimation. Simul Model Pract Th 2011; 19: 271-282.

[18] Vaez-Zadeh S, Harooni SR. Decoupling vector control of single-phase induction motor drives. In: IEEE 2005 36th Conference on Power Electronics Specialists; 12–18 June 2005; Recife, Brazil. New York, NY, USA: IEEE. pp. 733-738.

[19] Reicy S, Vaez-Zadeh S. Vector control of single-phase induction machine with maximum torque operation. In: IEEE 2005 International Symposium on Industrial Electronics; 20–23 June 2005; Dubrovnik, Croatia. New York, NY, USA: IEEE. pp. 923-928.

[20] Jannati M, Idris NRN, Aziz MJA. A new method for RFOC of induction motor under open-phase fault. In: 39th Annual Conference of the IEEE Industrial Electronics Society; 10–13 November 2013; Vienna, Austria. New York, NY, USA: IEEE. pp. 2530-2535.

[21] Jang DH. Problems incurred in a vector-controlled single-phase induction motor, and a proposal for a vector-controlled two-phase induction motor as a replacement. IEEE T Power Electr 2013; 28: 526-536.

[22] Wolbank TM, Wohrnschimmel R. On-line stator winding fault detection in inverter fed induction motors by stator current reconstruction. In: 9th IEEE Conference on Electrical Machines and Drive; 1–3 September 1999; Canterbury, UK. New York, NY, USA: IEEE. pp. 253-257.

[23] Tallam RM, Habetler TG, Harley RG. Transient model for induction machines with stator winding turn faults. IEEE T Ind Appl 2002; 38: 632-637.

[24] Tallam RM, Habetler TG, Harley RG, Gritter DJ, Burton BH. Neural network based on-line stator winding turn fault detection for induction motors. In: IEEE 2000 Conference Record of the Industry Applications; 8–12 October 2000; Rome, Italy. New York, NY, USA: IEEE. pp. 375-380.

[25] Zidani F, Diallo D, Benbouzid MEH, Naït-Saïd R. A fuzzy-based approach for the diagnosis of faults modes in a voltage-fed PWM inverter induction motor. IEEE T Ind Electron 2008; 55: 586-593.

[26] Diallo D, Benbouzid MEH, Hamad D, Pierre X. Fault detection and diagnosis in an induction machine drive: a pattern recognition approach based on Concordia stator mean current vector. IEEE T Energy Conver 2005; 20: 512-519.

[27] Gaeta A, Scelba G, Consoli A. Sensorless vector control of PM synchronous motors during single-phase open-circuit faulted conditions. IEEE T Ind Appl 2012; 48: 74-83.

[28] Gaeta A, Scelba G, Consoli A. Modelling and control of three-phase PMSMs under open-phase fault. IEEE T Ind Appl 2013; 49: 1968-1979.

[29] Bellini A, Filippetti F, Tassoni C, Capolino GA. Advances in diagnostic techniques for induction machines. IEEE T Ind Electron 2008; 55: 4109-4126.

[30] Krause PC. Analysis of Electric Machinery. New York, NY, USA: McGraw-Hill, 1986.

[31] Asgari SH, Jannati M, Idris NRN. Modeling of three-phase induction motor with two stator phases open-circuit. In: IEEE 2014 Conference on Energy Conversion; 13–15 October 2014; Johor Bahru, Malaysia. New York, NY, USA: IEEE. pp. 231-236.

Appendix A

From Eqs. (3a)–(3e), the following matrices are obtained:

$$\begin{aligned} v_{ds}^{s} &= \begin{bmatrix} 1 & j \end{bmatrix} \begin{bmatrix} v_{x_1 s}^{s} \\ v_{y_1 s}^{s} \end{bmatrix}, \quad i_{ds}^{s} = \begin{bmatrix} 1 & j \end{bmatrix} \begin{bmatrix} i_{x_1 s}^{s} \\ i_{y_1 s}^{s} \end{bmatrix} \\ v_{dr}^{s} &= \begin{bmatrix} 1 & j \end{bmatrix} \begin{bmatrix} v_{x_1 r}^{s} \\ v_{y_1 r}^{s} \end{bmatrix}, \quad i_{dr}^{s} = \begin{bmatrix} 1 & j \end{bmatrix} \begin{bmatrix} i_{x_1 r}^{s} \\ i_{y_1 r}^{s} \end{bmatrix} \end{aligned},$$

which gives:

$$\begin{bmatrix} F^{s} \\ jF^{s} \end{bmatrix} = \begin{bmatrix} 1 & j \\ j & -1 \end{bmatrix} \begin{bmatrix} A_{x_1 s}^{s} \\ A_{y_1 s}^{s} \end{bmatrix}.$$

In the above equation, F can be voltage or current vector. Therefore:

$$\begin{bmatrix} -F^{s} \\ jF^{s} \end{bmatrix} = \begin{bmatrix} -1 & -j \\ j & -1 \end{bmatrix} \begin{bmatrix} A_{x_1 s}^{s} \\ A_{y_1 s}^{s} \end{bmatrix}.$$

Using the following substitutions:

$$\begin{aligned} -F^{s} &\rightarrow F_{ds}^{e}, \quad & jF^{s} &\rightarrow F_{qs}^{e} \\ -1 &\rightarrow \cos\theta_e, \quad & -j &\rightarrow \sin\theta_e \\ A_{x_1 s}^{s} &\rightarrow F_{ds}^{s}, \quad & A_{y_1 s}^{s} &\rightarrow F_{qs}^{s} \end{aligned}$$

Eq. (9) is obtained.

$$\begin{bmatrix} F_{ds}^{e} \\ F_{qs}^{e} \end{bmatrix} = \underbrace{\begin{bmatrix} \cos\theta_e & \sin\theta_e \\ -\sin\theta_e & \cos\theta_e \end{bmatrix}}_{[T_s^e]} \begin{bmatrix} F_{ds}^{s} \\ F_{qs}^{s} \end{bmatrix}$$

Appendix B

Conventional RFOC method for 3-phase IM:

In the indirect RFOC method, since the slip command forces to zero asymptotically, the rotor flux vector is quickly aligned to the d-axis and this gives: $\begin{aligned} \lambda_{dr}^{mr} &= |\lambda_{dr}| \\ \lambda_{qr}^{mr} &= 0 \end{aligned}$.

In these equations the superscript "mr" indicates that the equations are in the rotating reference frame. Using this assumption, the equation for rotor flux can be written as [6]:

$$\begin{bmatrix} |\lambda_r| \\ 0 \end{bmatrix} = \begin{bmatrix} M & 0 \\ 0 & M \end{bmatrix} \begin{bmatrix} i_{ds}^{mr} \\ i_{qs}^{mr} \end{bmatrix} + \begin{bmatrix} L_r & 0 \\ 0 & L_r \end{bmatrix} \begin{bmatrix} i_{dr}^{mr} \\ i_{qr}^{mr} \end{bmatrix}.$$

From this equation the rotor currents in the rotor field oriented frame are obtained as:

$$\begin{aligned} i_{dr}^{mr} &= \tfrac{|\lambda_r|}{L_r} - \tfrac{M}{L_r} i_{ds}^{mr} \\ i_{qr}^{mr} &= -\tfrac{M}{L_r} i_{qs}^{mr} \end{aligned}.$$

Therefore, the complete equations of the 3-phase IM in the rotor field oriented frame can be written as follows [6]:

$$v_{ds}^{mr} = r_s i_{ds}^{mr} + L'_s \frac{d}{dt} i_{ds}^{mr} - \omega_{mr} L'_s i_{qs}^{mr} + (L_s - L'_s) \frac{d}{dt} (\frac{|\lambda_r|}{M}),$$

$$v_{qs}^{mr} = r_s i_{qs}^{mr} + L'_s \frac{d}{dt} i_{qs}^{mr} - \omega_{mr} L'_s i_{ds}^{mr} + \omega_{mr} (L_s - L'_s) (\frac{|\lambda_r|}{M}),$$

$$T_r \frac{d}{dt} |\lambda_r| + |\lambda_r| - M i_{ds}^{mr} = 0,$$

$$T_r (\omega_{mr} - \omega_r) |\lambda_r| - M i_{qs}^{mr} = 0,$$

$$\tau_e = \frac{P}{2} \times \frac{M}{L_r} \times |\lambda_r| \times i_{qs}^{mr},$$

where:

$$T_r = \frac{L_r}{r_r} \quad , \quad L'_s = L_s - \frac{M^2}{L_r} \quad , \quad L_s = L_{ls} + \frac{3}{2} L_{ms} \quad , \quad M = \frac{3}{2} L_{ms}.$$

In the above equations, the stator d-q voltages from the decoupler block and PI blocks are obtained as follows:

$$v_{ds}^{d} = -\omega_{mr} L'_s i_{qs}^{mr},$$

$$v_{qs}^{d} = \omega_{mr} L'_s i_{ds}^{mr} + \omega_{mr} (L_s - L'_s) (\frac{|\lambda_r|}{M}),$$

$$v_{ds}^{ref} = r_s i_{ds}^{mr} + L'_s \frac{d}{dt} i_{ds}^{mr} + (L_s - L'_s) \frac{d}{dt} (\frac{|\lambda_r|}{M}),$$

$$v_{qs}^{ref} = r_s i_{qs}^{mr} + L'_s \frac{d}{dt} i_{qs}^{mr}.$$

Finally, the equations of conventional RFOC for a healthy 3-phase IM can be summarized as follows:

Flux equation	$\|\lambda_r\| + T_r \frac{d\|\lambda_r\|}{dt} = M i_{ds}^{mr}$
Torque equation	$\tau_e = \frac{P}{2} \times \frac{M}{L_r} \times \|\lambda_r\| \times i_{qs}^{mr}$
Speed equation	$\omega_{mr} = \omega_r + \frac{M i_{qs}^{mr}}{T_r \|\lambda_r\|}$
Stator d-axis voltage equation	$v_{ds}^{mr} = -\omega_{mr} L'_s i_{qs}^{mr} + r_s i_{ds}^{mr} + L'_s \frac{d}{dt} i_{ds}^{mr} + (L_s - L'_s) \frac{d}{dt} (\frac{\|\lambda_r\|}{M})$
Stator q-axis voltage equation	$v_{qs}^{mr} = \omega_{mr} L'_s i_{ds}^{mr} + \omega_{mr} (L_s - L'_s) (\frac{\|\lambda_r\|}{M}) + r_s i_{qs}^{mr} + L'_s \frac{d}{dt} i_{qs}^{mr}$

Appendix C

The ratings and parameters of 3-phase IM:

Voltage: 400 V, f = 50 Hz, No. of poles = 4, Power = 1500 W, $J = 0.0086$ kgm^2, $r_s = 5.5\ \Omega$, $L_{lr} = L_{ls} = 0.0314$ H, $r_r = 6.5\ \Omega$, $M = 0.851$ H.